EPJ Web of Conferences **63**, 01012 (2013)
DOI: 10.1051/epjconf/ 20136301012

Shape evolution and Gamow-Teller β-decay of neutron-rich A∼100 nuclei within beyond-mean-field approach

A. Petrovici[1,a]

[1] *National Institute for Physics and Nuclear Engineering - Horia Hulubei, R-077125 Bucharest, Romania*

Abstract. Neutron-rich nuclei in the A∼100 mass region manifest drastic changes in some isotopic chains and sudden variations of particular nuclear properties with increasing spin and excitation energy. Our recent investigations represent an attempt to the self-consistent description of exotic phenomena in neutron-rich A∼100 nuclei within the *complex* Excited Vampir model using a realistic effective interaction in a large model space. Triple shape coexistence and shape evolution in the N=58 Sr and Zr isotopes as well as Gamow-Teller β-decay of ^{102,104}Tc nuclei are discussed.

1 Introduction

The structure of neutron-rich nuclei in the A∼100 mass region relevant for the r-process as well as reactor decay heat manifests drastic changes in some isotopic chains and often sudden variations of particular nuclear properties have been identified.

Neutron-rich Sr and Zr nuclei indicate rapid transition from spherical to deformed shape with a possible identification of the sudden onset of quadrupole deformation increasing the neutron number from N = 58 to N = 60. We investigated the structural changes and the evolution of deformation with increasing spin aiming at a unitary description of the lowest few 0^+ states and the low, intermediate, and high spins in ^{96}Sr and ^{98}Zr.

Of high interest in nuclear technology are the Gamow-Teller β-decay properties of some neutron-rich A∼100 nuclei responsible for about 6%-8% of the reactor decay heat during the operation and for essentially most of the energy after shutdown. We studied the Gamow-Teller β-decay strength distributions for ^{102,104}Tc, two important contributors to the decay heat in the nuclear reactors.

The shape coexistence phenomena specific for the investigated nuclei are discussed in the frame of the *complex* Excited Vampir (EXVAM) beyond-mean-field approach. Coexistence phenomena characterizing the structure and dynamics of proton-rich A∼70 nuclei have been successfully explained within this variational model [1–4]. The model uses Hartree-Fock-Bogoliubov (HFB) vacua as basic building blocks and the underlying HFB transformations are essentially *complex* and do mix proton- with neutron-states as well as states of different parity and angular momentum. The broken symmetries (nucleon numbers, parity, total angular momentum) are restored by projection techniques and the resulting symmetry-projected configurations are used as test wave functions in chains of successive variational calculations to determine the underlying HFB transformations as well as the configuration mixing. The rather large model space above the ^{40}Ca core is built out of $1p_{1/2}$, $1p_{3/2}$, $0f_{5/2}$, $0f_{7/2}$, $2s_{1/2}$, $1d_{3/2}$, $1d_{5/2}$, $0g_{7/2}$, $0g_{9/2}$, and $0h_{11/2}$ oscillator orbits for both protons and neutrons in the valence space. The corresponding single-particle energies had been adjusted in *complex* MONSTER (VAMPIR) calculations for odd-mass nuclei. The effective two-body interaction is constructed from a nuclear matter G-matrix based on the Bonn A potential and the Coulomb interaction between the valence protons is added [5, 6].

2 Triple shape coexistence and shape evolution in ^{96}Sr and ^{98}Zr

We calculated the lowest positive parity states up to spin 20^+ in ^{96}Sr and ^{98}Zr including in the Excited Vampir many-nucleon bases up to 12 EXVAM configurations. The final solutions for each spin have been obtained diagonalizing the residual interaction between the considered Excited Vampir configurations. For each nucleus the calculated states have been organized in bands based on the B(E2;ΔI = 2) values connecting them. The theoretical lowest bands of ^{96}Sr and ^{98}Zr are compared to the experimental data [7–11] in figures 1 and 2, respectively. The states building the $po(p)$-band in each nucleus are characterized by strong prolate-oblate mixing at low spins and variable prolate mixing at intermediate and high spins. At intermediate and high spins prolate and oblate bands coexist in both nuclei. A particular situation is found for the 0^+ states: the lowest projected EXVAM configuration is spherical in both nuclei (the quadrupole deformation parameter amounts to $\beta_2 \simeq 0.03$). In ^{96}Sr the second 0^+ configuration is oblate deformed in the intrinsic system

[a] e-mail: spetro@nipne.ro

Table 1. Structure of wave functions for 0^+ states.

	^{96}Sr			^{98}Zr		
I[$\hbar$]	sph	prol	obl	sph	prol	obl
0^+_1	36%	20%	44%	12%	43%	45%
0^+_2	57%	18%	25%	84%	12%	4%
0^+_3		69%	31%	1%	57%	42%
0^+_4	4%	6%	90%	2%	10%	88%

(β_2 = -0.32), the third one is prolate (β_2 = 0.37) and all three orthogonal configurations are situated in an energy interval of 375 keV. In ^{98}Zr the second configuration is prolate (β_2 = 0.37), the third is oblate (β_2 = -0.30) and the separation energy between the spherical one and the third one is 323 keV. The structure of the lowest four 0^+ states in terms of spherical, prolate, and oblate content is presented in table 1. Support for the mixing of configurations with different intrinsic deformations in the structure of the wave functions for the 0^+ states is offered by the strong $\rho^2(E0)$ values found theoretically and experimentally in both nuclei. The results concerning the oblate-prolate mixing in the structure of the wave functions for the lowest two 2^+ and 4^+ states is illustrated in table 2. Recent experimental results give support to the theoretical oblate-prolate mixing: the spectroscopic quadrupole moment of the 2^+_1 state in ^{96}Sr is equal 0 [11] while the calculated value is $Q^{spec}(2^+_1) = 9.5\ efm^2$ using the effective charges e_p = 1.3 and e_n = 0.3. The experimental B(E2) values for the transitions connecting the lowest 0^+ and 2^+ states in ^{96}Sr support the idea of strong shape mixing. The retardation of the $2^+_1 \rightarrow 0^+_1$ transition is induced from the strength B(E2) = 340 (209) e^2fm^4 deduced from the measured lifetime of 7(4) ps [10]. Recently reported experimental results indicate for this lifetime 4.1 ps [11] in agreement with the EXVAM predictions for the corresponding strength: $B(E2; 2^+_1 \rightarrow 0^+_1)$=795 e^2fm^4 in ^{96}Sr and 1140 e^2fm^4 in ^{98}Zr. In agreement with the available data [8] the theoretical results indicate deformation and significant fragmentation of the E2 strength decaying a given state due to the high density of states obtained at intermediate and high spins in both nuclei. The evolution of the structural changes is correlated with the faster alignment of the neutrons in $0h_{11/2}$ with respect to the protons in $0g_{9/2}$ within the $po(p)$-band while similar alignment is manifested by the neutrons and protons occupying these orbitals along the o-band in both nuclei. Consequently, the g-factor values of the $I^\pi \geq 8^+$ states along the $po(p)$-band are smaller ($\simeq$ 0.24 in ^{96}Sr and $\simeq$ 0.14 in ^{98}Zr) than the predicted values for the $I^\pi \geq 10^+$ states along the o-band (0.5 (0.44) in ^{96}Sr (^{98}Zr)).

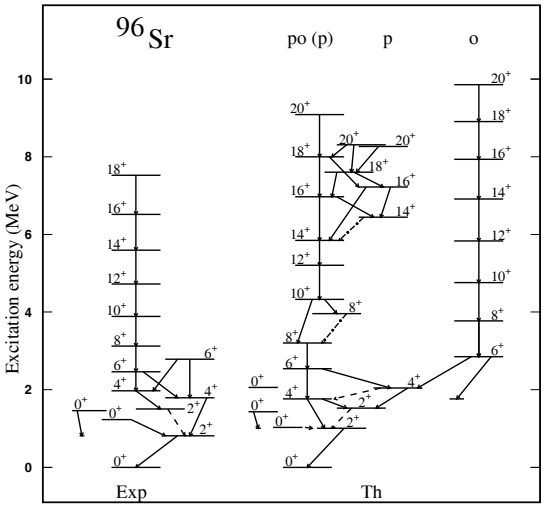

Figure 1. Theoretical EXVAM spectrum of ^{96}Sr compared to experimental data [7–9].

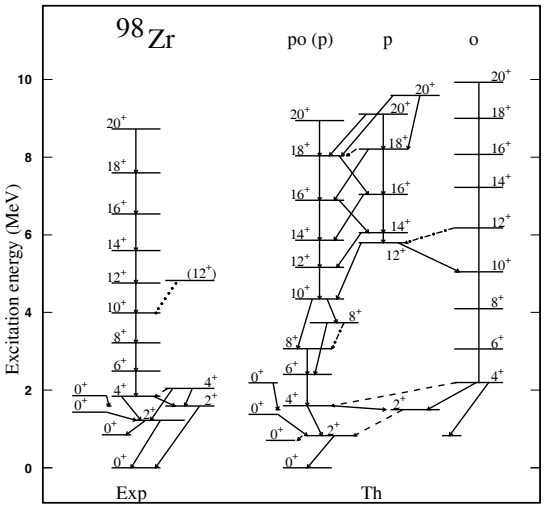

Figure 2. Theoretical EXVAM spectrum of ^{98}Zr compared to experimental data [7–9].

Table 2. The o-p mixing of lowest 2^+ and 4^+ states.

	^{96}Sr		^{98}Zr	
I[$\hbar$]	o-mixing	p-mixing	o-mixing	p-mixing
2^+_1	58(5)%	34(2)%	31%	60(8)%
2^+_2	33(2)%	65%	63(1)%	36%
4^+_1	36(6)%	56(1)%	10%	83(7)%
4^+_2	52(5)%	43%	85(1)%	13(1)%

3 Gamow-Teller β-decay of ^{102,104}Tc

The Gamow-Teller (GT) β decay of neutron-rich A$\sim$100 nuclei is not only relevant to nuclear structure, but is of high interest in nuclear technology. The estimation and control of the heat emitted by the decay of fission products requires certain still missing useful information, such as a knowledge of the decay properties of specific nuclei that contribute to the heating of the reactor during and after operation [12]. The precise and reliable description of the lowest states of the parent nucleus and of the states in the β window in the daughter nucleus necessary for a good description of the Gamow-Teller β-decay properties is a more difficult task for nuclei dominated by shape coexistence and mixing. Our recent self-consistent investigation

Table 3. The amount of mixing of the GT-contributing lowest states of ^{102}Ru.

0^+-states		2^+-states	
oblate	prolate	oblate	prolate
23%	74%	33%	66%
64%	33%	69%	29%
13%	85%	36%	61%
29%	70%	72%	26%
42%	55%	56%	42%
72%	26%	20%	78%
39%	60%		
26%	73%		
39%	59%		

Table 4. The amount of mixing of the GT-contributing lowest states of ^{104}Ru.

2^+-states		4^+-states	
oblate	prolate	oblate	prolate
27%	72%	67%	32%
77%	20%	38%	61%
89%	9%	89%	8%
16%	82%	3%	96%
82%	16%	45%	53%
38%	61%	63%	37%
61%	38%		
68%	30%		
79%	19%		

of the Gamow-Teller strength distributions, β-decay half-lives, and β-delayed neutron emission probabilities for ^{104}Zr and ^{106}Zr nuclei within the *complex* Excited Vampir model [13] indicated good agreement with the experimental data [14] . Recently have been published the first results of the total absorption gamma spectrometer (TAGS) measurements of nuclei that are important contributors to the decay heat in nuclear reactors and the self-consistent description of their Gamow-Teller β decay properties [15]. In the frame of the *complex* Excited Vampir model we investigated for the first time the Gamow-Teller strength distributions and accumulated strengths for the β-decay of ^{102}Tc to ^{102}Ru and of ^{104}Tc to ^{104}Ru. We calculated the lowest 1^+ states in ^{102}Tc, the lowest 3^+ states in ^{104}Tc, and the positive-parity states up to spin 4^+ in ^{102}Ru and ^{104}Ru. The obtained results indicate that the structure of the wave function for the lowest 1^+ state of ^{102}Tc manifest a strong mixing of differently deformed prolate and oblate configurations in the intrinsic system. Altogether the prolate components represent 53% of the total amplitude and the oblate components make 47% in the structure of the wave function while the wave function for the lowest 3^+ state of ^{104}Tc is dominated (99%) by a single prolate deformed configuration. The wave functions of the daughter states with significant Gamow-Teller strength manifest significant oblate-prolate mixing as it is illustrated in table 3 and table 4 for ^{102}Ru and ^{104}Ru, respectively.

Table 5. Spectroscopic quadrupole moments (in efm^2) of GT-contributing low-lying states of ^{102}Ru and ^{104}Ru.

^{102}Ru	^{104}Ru	
2^+-states	2^+-states	4^+-states
-19.2	-28.0	34.3
23.7	42.0	-17.0
-14.7	54.4	71.1
30.1	-44.0	-82.9
3.9	50.1	-7.6
-36.7	-10.5	23.7
	16.2	
	26.7	
	42.0	

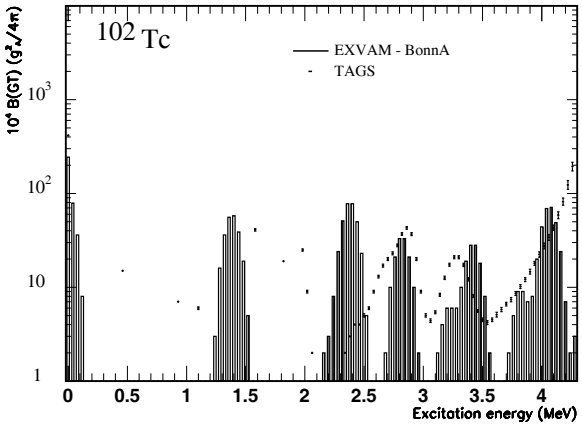

Figure 3. The Gamow-Teller strength distribution for the decay of ^{102}Tc obtained within the *complex* Excited Vampir model compared with TAGS results.

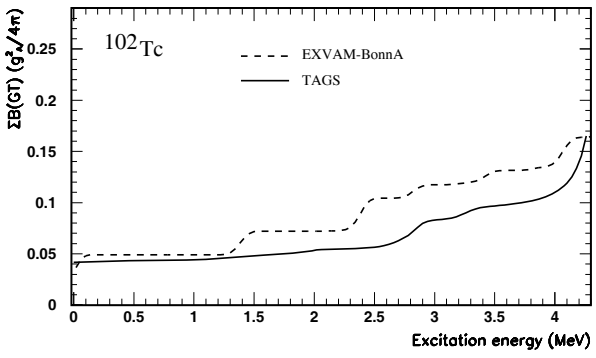

Figure 4. The accumulated GT strength for the decay of ^{102}Tc obtained within the *complex* Excited Vampir model compared with TAGS results.

The deformation of the main configurations in the structure of the wave functions is smaller in ^{102}Ru where the number of neutrons is the critical N = 58 [6] while in ^{104}Ru the larger deformation is determined by the neutron number N = 60. The corresponding spectroscopic quadrupole moments are presented in table 5.

To imitate the finite experimental resolution in the presentation of the data the theoretical results have been folded

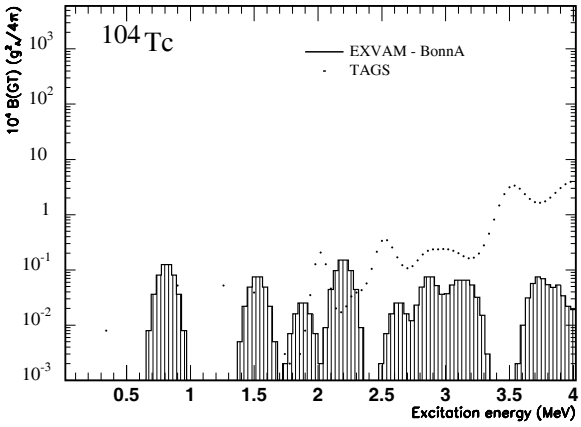

Figure 5. The GT strength distribution for the decay of ^{104}Tc obtained within the *complex* Excited Vampir model compared with TAGS data.

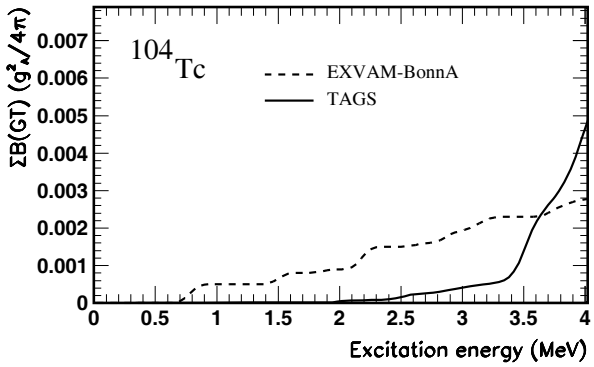

Figure 6. The accumulated GT strength for the decay of ^{104}Tc obtained within the *complex* Excited Vampir model compared with TAGS results.

with Gaussian functions whose width was taken from the experimental resolution of the TAGS. The folded theoretical results are the displayed as histogram with 40 keV bins.

The Gamow-Teller strength distribution for the decay of the 1^+ parent state in ^{102}Tc to the calculated 0^+ and 2^+ daughter states in ^{102}Ru is presented in figure 3 compared with TAGS results. The GT strength for the decay to the 1^+ states in ^{102}Ru is negligible. The corresponding accumulated Gamow-Teller strength is compared with the TAGS results in figure 4. The Gamow-Teller strength distribution for the decay of the 3^+ parent state in ^{104}Tc to the calculated 2^+ and 4^+ daughter states in ^{104}Ru (the 3^+ states do not have a significant contribution) is compared with TAGS results in figure 5 and the accumulated GT strength in figure 6.

The strong Gamow-Teller β-decay branches indicate essential contribution from the $g^{\pi}_{9/2}g^{\nu}_{7/2}$, $d^{\pi}_{5/2}d^{\nu}_{3/2}$, and $d^{\pi}_{5/2}d^{\nu}_{5/2}$ matrix elements. Smaller contributions are obtained from $p^{\pi}_{1/2}p^{\nu}_{3/2}$ and $p^{\pi}_{3/2}p^{\nu}_{1/2}$ matrix elements. In the decay of ^{102}Tc to ^{102}Ru the $g^{\pi}_{9/2}g^{\nu}_{7/2}$ contribution is large and the $d^{\pi}_{5/2}d^{\nu}_{3/2}$ is significant but smaller. From the matrix elements $d^{\pi}_{5/2}d^{\nu}_{5/2}$, $p^{\pi}_{1/2}p^{\nu}_{3/2}$, and $p^{\pi}_{3/2}p^{\nu}_{1/2}$ appear cancellations but they are significantly weaker. In the case of ^{104}Tc to ^{104}Ru decay the same matrix elements are relevant, but all of them are relatively small and the cancellations produce the final small strength for each Gamow-Teller contributing state.

In summary, the *complex* Excited Vampir model describes self-consistenty the multifaceted yrast structure of the N = 58 Sr and Zr isotopes predicting triple shape coexistence for the lowest 0^+ states and coexistence of prolate and oblate deformed bands at intermediate and high spins. The Excited Vampir results indicate that the specific mixing of prolate and oblate projected configurations in the structure of the parent state as well as the daughter states is responsible for the significant difference in the Gamow-Teller β-decay properties of the ^{102}Tc and ^{104}Tc nuclei.

Acknowledgments

This work was supported by a grant of the Romanian National Authority for Scientific Research, CNCS-UEFISCDI, project number PN-II-ID-PCE-2011-3-0153 and the CERN-ISOLDE contract 6/2012.

References

[1] A. Petrovici, K.W.Schmid, A. Faessler, Nucl. Phys. **A665**, 333 (2000)

[2] A. Petrovici, K.W. Schmid, O. Radu, A. Faessler, Phys. Rev. C **78**, 044315 (2008)

[3] A. Petrovici, K.W. Schmid, O. Radu, A. Faessler, *Phys. Rev.* C **78**, 064311 (2008)

[4] A. Petrovici, K.W. Schmid, O. Radu, A. Faessler, Phys. Rev. C **80**, 044319 (2009)

[5] A. Petrovici, K.W. Schmid, A. Faessler, J.Phys.:Conf. Series **312**, 092051 (2011)

[6] A. Petrovici, Phys. Rev. C **85**, 034337 (2012).

[7] G. Lhersonneau *et al.*, Phys. Rev. C **49**, 1379 (1994).

[8] W. Urban *et al.*, Nucl. Phys. **A689**, 605 (2001).

[9] C. Y. Wu *et al.*, Phys. Rev. C **70**, 064312 (2004).

[10] H. Mach *et al.*, Nucl. Phys. **A523**, 197 (1991).

[11] E. Clément *et al.*, CERN-INTC-2010-009/INTC-P-216-ADD-108/01/2010.

[12] A. Algora *et al.*, Phys. Rev. Lett. **105**, 202501 (2010).

[13] A. Petrovici, K. W. Schmid, and A. Faessler, Prog. Part. Nucl. Phys. **66**, 287 (2011).

[14] J. Pereira *et al.*, Phys. Rev. C **79**, 035806 (2009).

[15] D. Jordan *et al.*, Phys. Rev. C **87**, 044318 (2013).